# SMARTSCAN – hardware test results for smart optoelectronic image correction for pushbroom cameras

Valerij Tchernykh[a], Sergei Dyblenko[a], Klaus Janschek[a], Wolfgang Göhler[b], Bernd Harnisch[c]

[a]Technsiche Universität Dresden, Department of Electrical Engineering and Information Technology, D-01062 Dresden, Germany
[b]HTS GmbH, Am Glaswerk 3, D-01640 Coswig, Germany
[c]European Space Agency, ESTEC, 2201 AZ Noordwijk, The Netherlands

## ABSTRACT

The paper describes the test results of the hardware model of a smart pushbroom imaging system. The imaging system can be used on satellites with moderately attitude stability due to application of the image correction on base of the real-time image motion record by an optoelectronic image processor and auxiliary sensors in the focal plane. The tested model includes the breadboard model of a smart pushbroom camera with auxiliary sensors, the optoelectronic processor model and the image correction software. The tests have been performed on a laboratory satellite motion simulator based on a 5 DOF industrial robot. Numerical values of the image motion record accuracy and the image correction efficiency are given as well as a detailed test description.

Keywords: optoelectronic image correction, pushbroom cameras, optical correlator

## 1. INTRODUCTION

Pushbroom scan cameras with linear image sensors, commonly used for Earth observation from satellites, require high attitude stability during scan of the frame. For high resolution cameras, instant attitude changes by even less than one arc second will result in significant image distortion and blurring (for example: with 1 m ground sampling distance, one pixel corresponds to 0.3 arc second). Especially noticeable are the effects of high frequency attitude variations: micro shocks and vibrations, produced by momentum and reaction wheels operations, mechanically activated coolers, steering and deployment mechanics and other reasons. High attitude stability requirements are one of the main reasons of high complexity and cost of the Earth observation satellites.

To solve this problem the SMARTSCAN concept was proposed (Fig. 1), which consists of recording of the actual image motion in the focal plane of the camera during the frame acquisition and correction of the obtained image distortions posteriori on base of the record[1]. The record can be produced by geometrical transformations of the shift vectors between the subsequently generated images from auxiliary matrix image sensors in the focal plane. The shifts can be determined with subpixel accuracy by 2D correlations of the images. This approach has low dependency from the image content and is extremely noise-resistant, but requires large processing resources, practically impossible for onboard digital processor. To provide the required performance, it was proposed to determine the shifts with an optical 2D optoelectronic correlation processor.


Earth Observing Systems VII, William L. Barnes, Editor,
Proceedings of SPIE Vol. 4814 (2002) © 2002 SPIE · 0277-786X/02/$15.00

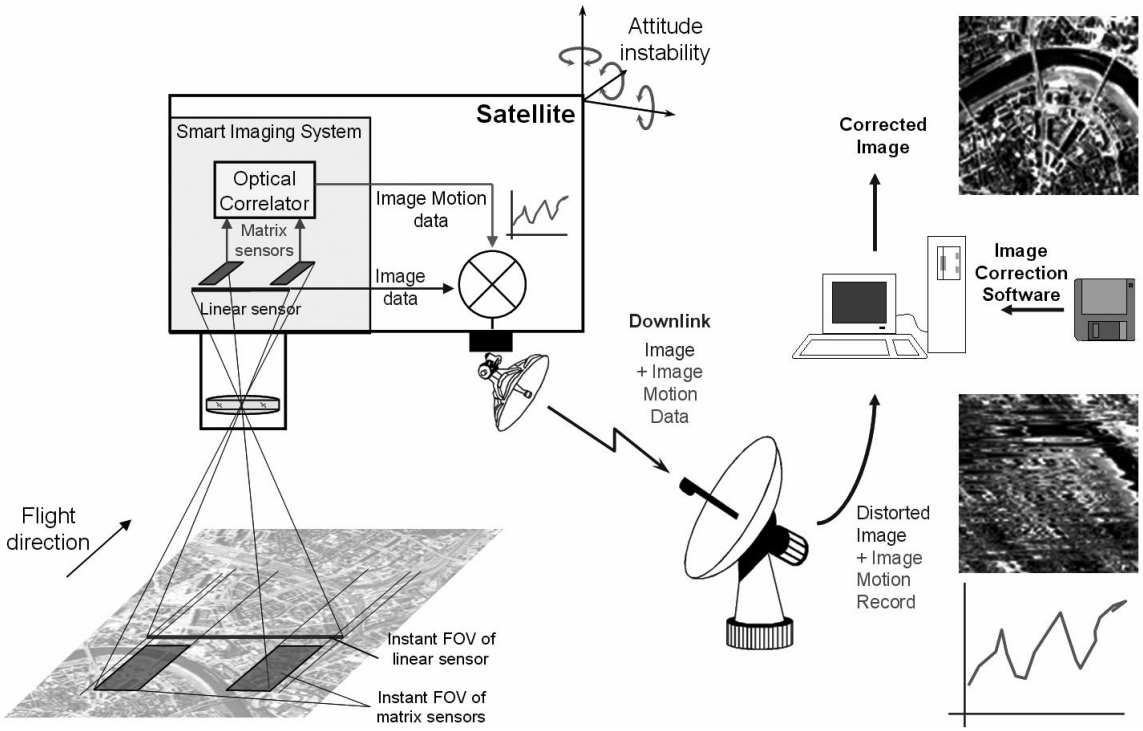


Fig. 1. SMARTSCAN imaging system concept

The optoelectronic processor is based on the scheme of a joint transform optical correlator[2], which performs the correlation of two input images by two sequential optical Fourier transforms with square law detection of the obtained Fourier spectrum images. As a result, a correlation image is formed. If the input images are of the same area and are overlapped, the correlation image contains two bright correlation peaks, where the mutual position of the peaks corresponds to the shift vector between the input images. The positions of the peaks are determined with subpixel accuracy and recalculated into the image shift vectors by a digital signal processor which can have a rather limited performance (due to massive data reduction after optical transformations).

To improve the mechanical robustness of the optical scheme, an innovative technique of self calibration has been proposed[3]. This technique makes the optoelectronic processor insensitive to mechanical deformations and in particular suitable for space applications.

With currently available optoelectronic components it is possible to process up to 10000 pairs of 64x64 pixels images per second. This allows to determine the position of the focal plane image for the moments of every line exposing (pushbroom scan satellite camera with 1 meter resolution produces approximately 3500 image lines per second).

The SMARTSCAN imaging system, comprising the smart pushbroom camera with auxiliary matrix image sensors, optoelectronic processor and the image correction software, accepts considerably large attitude disturbances without image quality degradation and will be therefore suitable for satellites with simplified attitude control. This allows using such smart pushbroom cameras (multi/hyper spectral) even on moderately stabilised platforms, e.g. small satellites, low earth orbit communication satellites or on manned space stations.

The SMARTSCAN imaging system concept has been successfully tested first with a hardware model of the optoelectronic processor and computer-generated images under ESA contract[4]. To test the system functionality with real images, a breadboard model of the smart pushbroom camera has been manufactured and mounted on a laboratory satellite motion simulator based on a 5 DOF industrial robot. The paper presents the detailed description and results of this test. Currently an airborne test is prepared to be conducted in July 2002.

## 2. TEST DESCRIPTION

### 2.1 Test facility

The SMARTSCAN system mock-up includes a breadboard model of the smart pushbroom camera, optoelectronic processor laboratory model, satellite motion simulator, test image, control and image correction software. The satellite motion is simulated by a 5-DOF industrial robot (Fig. 2). The camera model was mounted on the manipulator of the robot, which moved it over the test image simulating the orbital motion of the spacecraft and the attitude disturbances. The tests have been performed under control of a PC, which also performed the posteriori image correction and error determination.

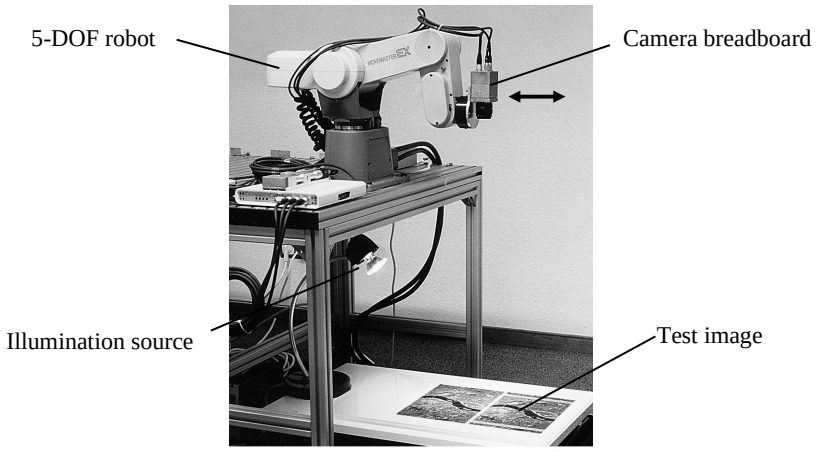


Fig. 2. Test facility

### 2.2 Attitude instability simulation

Roll angle oscillations with amplitudes of 0.1 - 0.2 degrees and a period of approximately one second were included in the preprogrammed trajectory. Instability of pitch and yaw angles was simulated by uncontrollable vibrations due to imperfections of robot. The average amplitude of the vibrations was approximately 0.1 degree on pitch and 0.01 – 0.04 degrees on yaw axis.

### 2.3 Optoelectronic processor model

The design of laboratory model of optoelectronic processor (Fig. 3) is based on scheme of the joint transform optical correlator[2].

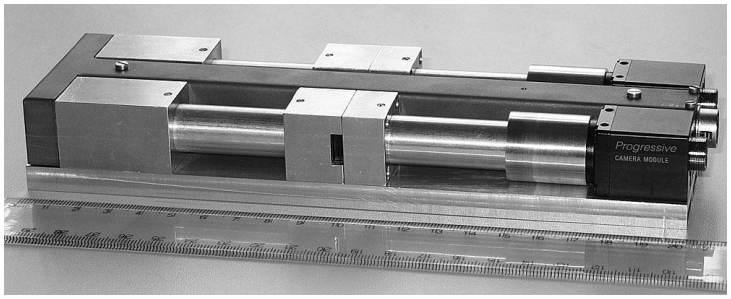


Fig. 3. Hardware model of the optoelectronic processor

The model employs the original self-calibration technique, which makes it insensitive to mechanical deformations[3]. To save the design and production cost, standard video cameras are used as image sensors, what limits the image processing rate by 60 correlations per second. Nevertheless, the model represents realistically the full performance optoelectronic processor in terms of accuracy. The model can determine the image shift within the range of ±280 pixels in the main image motion (scan) direction and ±140 pixels perpendicular to the scan direction.

### 2.4 Breadboard model of smart pushbroom camera

The model (Fig. 4) consists of the body, lens, focusing elements and the set of image sensors in the focal plane. The main image acquisition sensor is a linear one (as in standard pushbroom scan camera). Besides it, two auxiliary matrix sensors (small CCD cameras) are installed in the focal plane of the camera model.

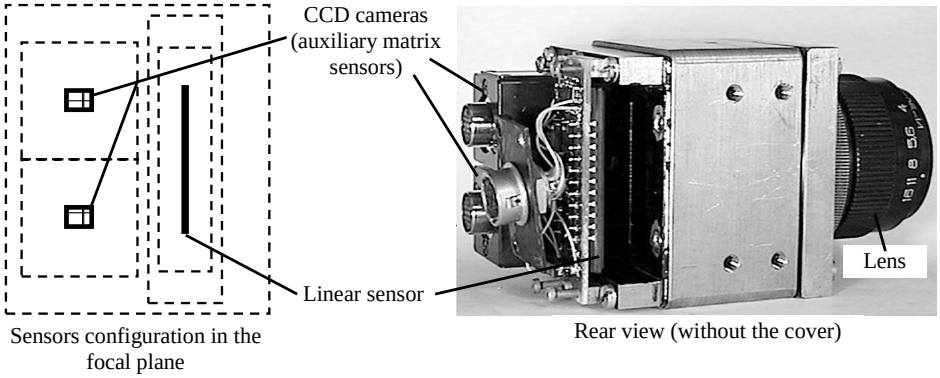


Fig. 4. Camera model

During the imaging operations, the linear sensor produced a large image frame (line by line, as a normal pushbroom scan camera). The auxiliary matrix sensors produced two sequences of small frames (video streams), which were processed in real time by the optoelectronic processor to produce the record of the focal plane image motion.

The main parameters of the model are:

1. Focal length of the lens … 75 mm
2. Matrix sensor image size … 640x480 pixels (fragments of 120x120 pixels were actually used for correlation)
3. Matrix sensors frame rate … 30 frames per second
4. Linear sensor image size … 2048 pixels wide; length limited only by storage (actually 2048 lines were recorded)
5. Linear sensor resolution … 187 μrad per pixel

### 2.5 Test image and reference image motion determination

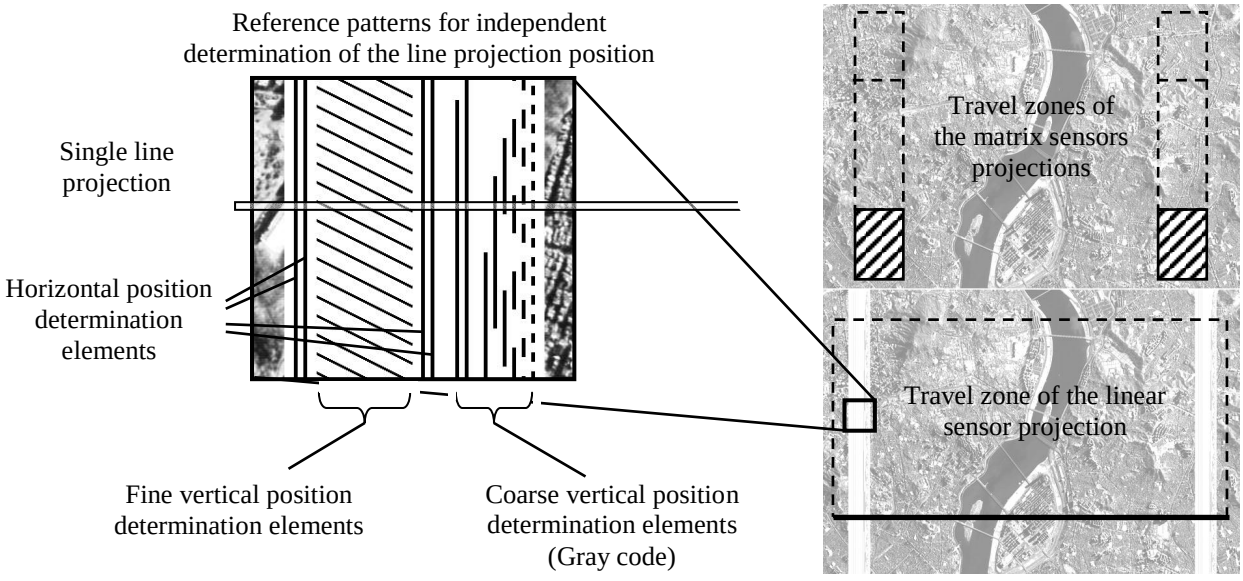


Fig. 5. Test image structure

The test image (Fig. 5) used for the laboratory tests is based on one of the demo images from the EROS satellite, published in Internet (http://www.imagesatintl.com/01_18_01.html). The original image shows Seoul, South Korea, at a resolution of 1.8 m/pixel and a size of 5315 x 5491 pixels. The image was duplicated to increase the size and to have approximately the same travel zones for matrix and linear sensor projections.

A special approach has been used to allow an independent determination of the focal plane image motion and to evaluate finally the image correction efficiency. For this purpose, special reference patterns have been included into the linear sensor travel zone. These patterns include vertical and inclined lines (Fig.4 left). Every image line taken by the linear sensor contained dark spots in the points of crossing with the pattern elements. The position of these spots within the line can be recalculated into the position of the line projection in the plane of test image. Vertical lines of the pattern were used to determine the horizontal position of the line; the vertical position was determined with the Gray code pattern (coarse) and inclined lines (fine).

The position coordinates of all the image lines form the reference image motion record. This reference record is generated completely independently from the optical processor record and can be compared therefore with it to evaluate the record accuracy and efficiency of the image correction.

### 2.7 Test procedure

The main data flows during the test are shown in Figure 6.

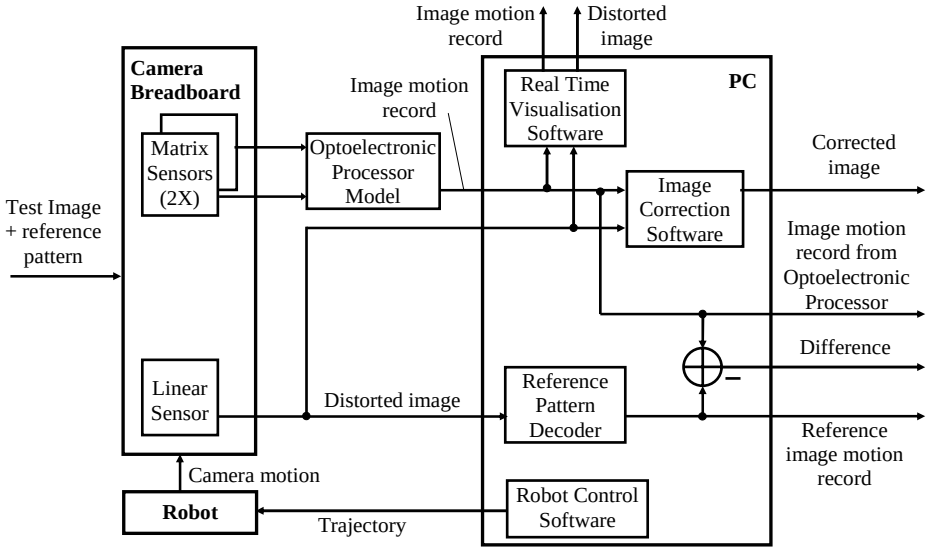


Fig. 6. Data flow chart

The trajectory of the camera motion for each test was generated by a PC and forwarded to the robot. The robot moved the camera breadboard on the pre-programmed trajectory. During the motion the linear sensor image was loaded in PC and visualized on the monitor in real time. The video streams from the auxiliary matrix sensors were processed in real time by the optoelectronic processor model, the result - image motion record – was also loaded to the PC and visualized. As the image motion range during the frame acquisition exceeds the maximum image shift, which can be measured by the optoelectronic processor directly (±280 pixels in scan direction), the image motion record is determined in few steps, with a certain accumulation of errors.

After finishing the image acquisition, the distorted linear sensor image has been corrected posteriori on base of the image motion record from the optoelectronic processor. The correction has been performed by calculation of the proper position of each obtained line in the coordinate frame of the corrected image and determination of the values of the corrected image pixel by interpolation of the neighboring distorted image pixels. The reference patterns were also processed to obtain the reference image motion record.

## 4. TEST RESULTS

### 4.1 Direct results of the test

As a result of the test, the distorted linear sensor image and the image motion record from the optoelectronic processor model (OPM) have been obtained (Figure 7). The reference image motion record has been determined in parallel by decoding of the reference patterns, included in the linear sensor image (see Fig. 5 left). The image motion records have been determined separately for left and right matrix image sensors and for left and right reference patterns (see test image structure - Fig. 5) to consider a possible image rotation. Figure 7 shows the OPM and reference records for left matrix sensor and left (bottom on fig. 5) reference pattern.

Fig. 7 shows also the ideal image motion record which corresponds in the scan direction to the case, when the focal plane image advances by exactly one pixel during one period of lines acquisition. Perpendicular to the scan direction the ideal record coincides with the horizontal axis, because in ideal case there should not be any image motion in this direction.

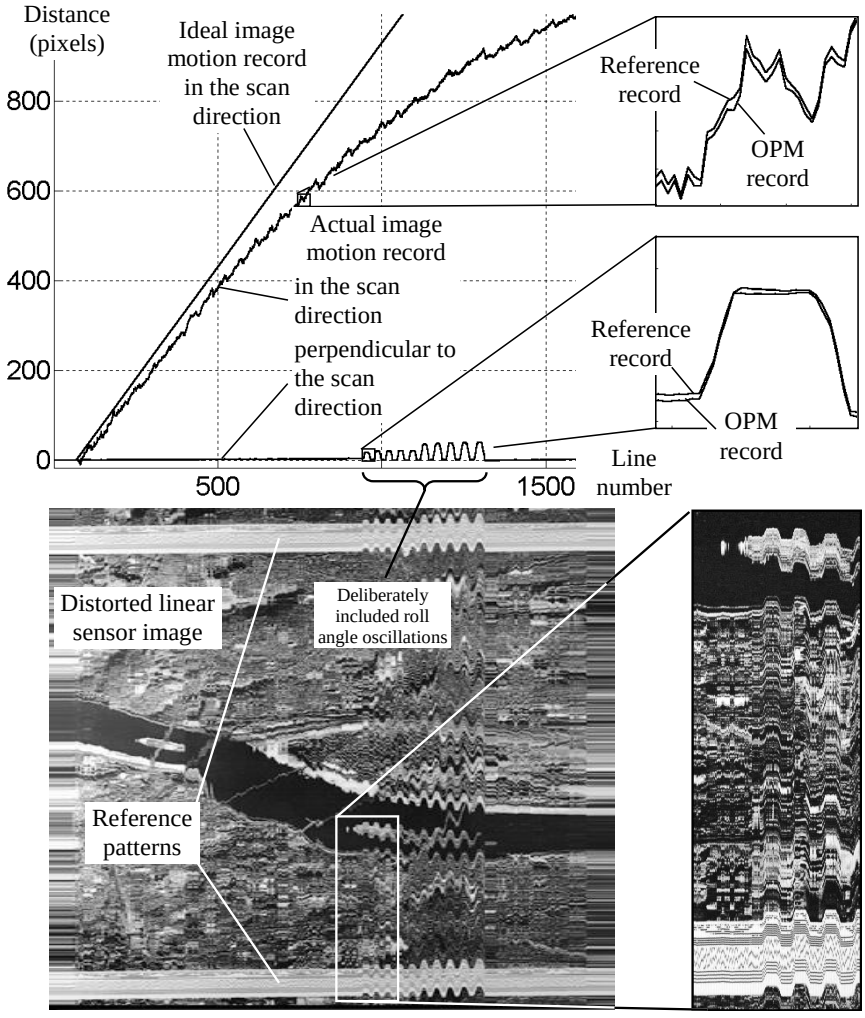


Fig. 7. Distorted image and image motion records

Image motion record from the optoelectronic processor and the reference record are very close. The difference between them represents the sum of errors of both records.

### 4.2 Errors analysis

*4.2.1 Static errors of optoelectronic processor*

Static tests of the optoelectronic processor were determined in separate test with fixed images. As a result, the random error of shift determination for different image texture types has been found to be within 0.1 pixels (1σ). This figure represents the additive component of the optoelectronic processor own error and does not consider the image acquisition-linked errors (discrete sampling effects, motion blur, optical distortions, etc.)

*4.2.2 Errors of the image motion record and their effect on the image correction*

The numerical errors of the image motion record were determined as a difference between the record from the optoelectronic processor and the reference record, obtained by decoding the reference patterns, included in the test image. This difference actually represents the sum of errors of both records and can be considered as the upper limit of the OPM record errors. Figure 8 shows the typical error curves for one of the OPM/reference record channels (left matrix sensor/left reference pattern).

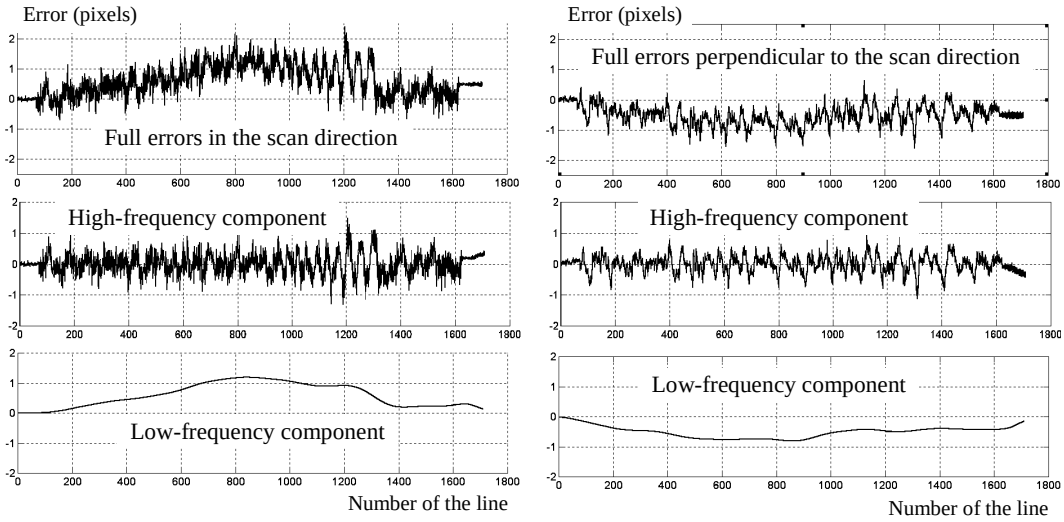


Fig. 8. Errors of the image motion records

To estimate the effect of the errors they have been subdivided into low frequency (including bias error) and high frequency components. The low frequency component was found to be within 0 … +1.5 pixels in the scan direction and within 0 … -1 pixel perpendicular to scan direction. After removal of the low frequency component, the RMS error of the image motion record was found to be σ= 0.36 pixels in the scan direction and σ= 0.28 pixels perpendicular to the scan direction.

Low frequency errors of the image motion record result in smooth residual distortions of the corrected image (smooth scale variations within the image). Within certain limits, such distortions are practically not visually detectable. They can only become noticeable, if the image will be used for precise distance measurements and if no previous observations or mapping has been made for the imaged area. Except for such applications smooth image distortions can be considered to be less significant for the image quality and considerably large amount of such distortions can be accepted.

High frequency errors of the image motion record result in sharp and very noticeable distortions of the corrected image and should therefore be minimised. During the tests, the value of these errors was found to be within σ= 0.3 …0.5 pixels, what is in principle acceptable for the good quality image correction.

The errors increase with respect to the static test results (σ<0.1 pixels) is at least partially caused by addition of the reference record errors and image blurring due to uncontrollable high amplitude shock and vibrations, produced by the industrial robot, which are not expected onboard the satellite. This allows to suggest even smaller errors for the real satellite application.

### 4.3 Image correction

The efficiency of the image correction has been estimated in two ways: numerically (by comparison of the image distortion values before and after correction) and visually (by visual comparison of the original, distorted and corrected images).

The image distortions here were understood as the difference between the ideal and actual positions of the focal plane image in the moments of every line acquisition (in ideal case the image advances by exactly one pixel during the period of the lines acquisition and does not move perpendicular to the scan direction). Therefore, the distortions before the correction can be interpreted as the difference between the ideal and the reference image record, residual distortions after correction – as the difference between OPM and reference records (Figure 9).

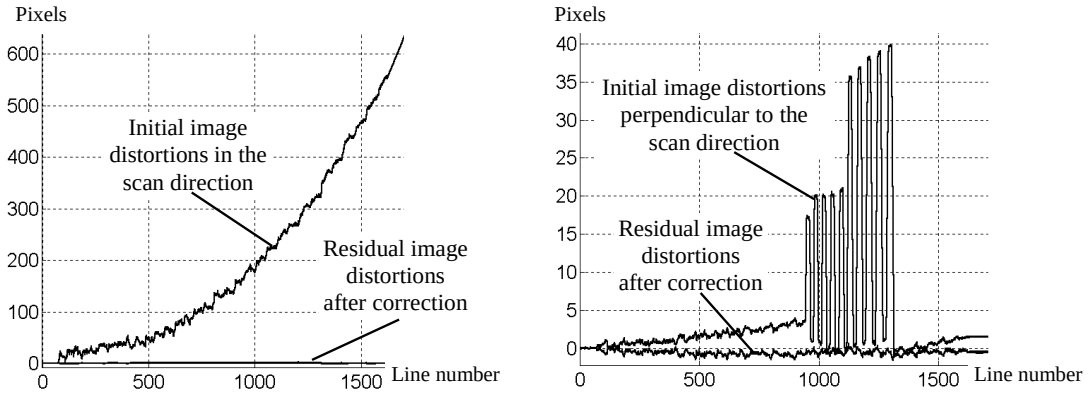


Fig. 9. Efficiency of the image distortion correction

Residual distortions demonstrated to have little dependency on the initial distortions value, so the maximum initial/residual distortions ratio was observed at maximum initial distortions, where the distortion suppression coefficient reached 20 … 50 times perpendicular to the image scan and over 500 in the scan direction.

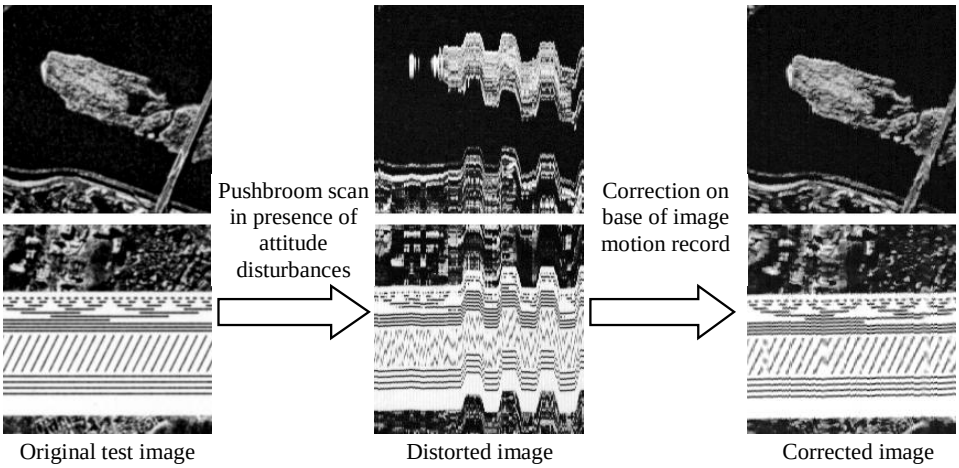


Fig. 10. Magnified fragments of original, distorted and corrected images

Figure 10 illustrated the results of the image correction. Visible breaks in the corrected image (better visible on the reference pattern fragment) were caused by uncontrollable shocks of the industrial robot with very high instant image velocity. As a result, there were large gaps between the neighboring lines from the linear sensor, for which no image information was available. Nevertheless, the geometrical correction was performed accurately – each line was placed in the proper place. The interpolation program used the nearest available image data to fill the gap. Such shocks are in any case not expected onboard the satellite.

Certain smoothing and residual distortions on the corrected image have three main sources:

- motion blur due to high instant image velocity;
- smoothing as a result of interpolation procedure itself;
- errors of the image motion record.

## 5. FOLLOW-ON TEST ACTIVITIES

### 5.1 Airborne testing

Airborne testing of the SMARTSCAN breadboard model will be performed in July 2002 using a Cessna Grand Caravan aircraft from DLR. The tests will prove the end-to-end functionality of the system under harsh attitude disturbances conditions (short-term attitude stability of the small turboprop aircraft is expected to be few orders of magnitude worse, compared to an observation satellite). The system will provide high resolution linear sensor images (2048x2048 pixels, 0.5 m/pixels) and real time records of the focal plane image motion. Besides that, a specially manufactured data recorder will record all data from the linear and matrix image sensors of the camera breadboard, which allows to perform the laboratory simulations of the airborne test with real image data.

### 5.2 Space verification

Different opportunities for a space verification of the SMARTSCAN system currently are examined. For this, a space compatible model of smart camera with optical correlator should be manufactured. Two main options are considered: installation on one of the exposed palettes of ISS (medium resolution imaging system with multispectral capability) or onboard a nanosatellite (low resolution panchromatic imaging).

## 6. CONCLUSIONS

As a result of the test, the functionality of the proposed SMARTSCAN imaging system was proved using real images from the camera breadboard. Pushbroom scan images, distorted as the result of the applied attitude instability, were successfully corrected on base of the image motion record, produced by optoelectronic processor model by real time processing of the video streams from the auxiliary matrix image sensors in the focal plane of the camera.

The overall errors of the image motion record are found to be 0.3 … 0.5 pixels ($1\sigma$, high frequency component) and within 2 pixels (low frequency component).

The efficiency of the image motion correction (distortion reduction coefficient) was between 20 and 500.

## ACKNOWLEDGEMENTS

This research was supported by ESA/ESTEC Contract No. 14858/00/NL/PB

## REFERENCES

1. K. Janschek, V. Tchernykh, S. Dyblenko, "Design concept for the secondary-payload Earth observation camera", in *Sensors, Systems and Next-Generation Satellites III*, Hiroyuki Fujisada, Joan B. Lurie, Editors, Proceedings of SPIE Vol. 3870, 78-86 (1999).
2. Jutamulia S. “Joint transform correlators and their applications”, *Proceedings SPIE*, **1812**, pp. 233-243, 1992.
3. V. Tchernykh, K. Janschek, S. Dyblenko. Space application of a self-calibrating optical processor for harsh mechanical environment. Proceedings of 1st IFAC –Conference on Mechatronic Systems, 18-20 Sept. 2000, Darmstadt, Germany.
4. V. Tchernykh, S. Dyblenko, K. Janschek, B. Harnisch, “Optical-correlator-based system for the real-time analysis of image motion in the focal plane of an Earth observation camera”, in *Algorithms and Systems for Optical Information Processing IV*, Bahram Javidi; Demetri Psaltis; Editors, Proceedings of SPIE Vol. 4113, 23-31 (2000).